HHS Public Access

Author manuscript

J Neurosci Res. Author manuscript; available in PMC 2017 December 01.

Published in final edited form as:

J Neurosci Res. 2017 June ; 95(6): 1330–1335. doi:10.1002/jnr.23883.

Topography of microglial activation in sensory and affect related brain regions in chronic pain

Anna M.W. Taylor[1], **Sadaf Mehrabani**[1], **Steve Liu**[2], **Alison J. Taylor**[1], and **Catherine M Cahill**[2]

[1]Department of Psychiatry and Biobehavioral Sciences, University of California, Los Angeles

[2]Department of Anesthesiology and Perioperative Care, University of California, Irvine

Abstract

Microglial activation in the spinal cord plays a central role in the development and maintenance of chronic pain following a peripheral nerve injury. To date, there has not been a thorough assessment of microglial activation in brain regions associated with pain and reward. To this end, we used a mouse model of neuropathic pain, whereby the left sciatic nerve of male C57Bl/6J mice was loosely constricted (chronic constriction injury) and assessed microglial activation in several brain regions two weeks following injury, a time point where pain hypersensitivity is well established. We found significant microglial activation in brain regions associated with sensory pain transmission and affect, including the thalamus, prefrontal cortex, and amygdala. Activation was consistently most robust in brain regions contralateral to the side of injury. Brain regions not directly involved in either the sensory of affective dimensions of pain, such as the motor cortex, did not display microglial activation. This study confirms that peripheral nerve injury induces microglial activation in regions involved with both sensory and affective components of pain.

Graphical Abstract

A peripheral nerve injury induces widespread microglial activation in brain regions associated with pain and affect. Activation was generally more pronounced on the contralateral side, corresponding to the region receiving input from injured afferents.

Corresponding Author: Anna M.W. Taylor, PhD, Department of Psychiatry and Biobehavioral Sciences, University of California, Los Angeles, 675 Charles E Young Drive South, Los Angeles, California 90095, (310) 206-7883, ataylor1@ucla.edu.

Conflict of Interests

The authors declare no conflict of interest.

Author Role

AMWT and CMC conceived and designed the experiments, SL performed the qRTPCR, AT, SM, and AMWT performed the immunocytochemistry and analysis, and AMWT and CMC wrote the manuscript.

Keywords

Neuropathic pain; affect; inflammation; microglia activation; brain; RRID:AB_839506

Introduction

Chronic non-cancer pain is defined as pain that persists for greater than 3 months, often in the absence of overt tissue damage (IASP, 1994). It is characterized by spontaneous ongoing pain and heightened sensitivity to innocuous and painful stimuli. Microglia, the resident immune cells of the central nervous system, are a critical player in the development of pain hypersensitivities that characterize chronic pain. Various animal models of chronic pain exhibit significant microglial activation in the superficial dorsal horn of the spinal cord, which directly contributes to the hypersensitivity of nociceptive afferents (Keller et al, 2007; Tsuda and Inoue, 2015). Blocking microglial activation alleviates pain hypersensitivity in several animal models of chronic pain (Raghavendra et al, 2003; Ledeboer et al, 2005; Mika et al, 2010).

Chronic pain conditions are also accompanied by significant affective and mood disorders, including depression and anxiety (Nicholson and Verma, 2004; Juurlink et al, 2004; Asmundson and Katz, 2009; Elman et al, 2013). Microglial activation has been reported in brain regions of patients with major depressive disorder, and preclinical studies have shown to contribute to the progression and severity of these conditions (Bhattacharya et al, 2016, for review). While there have been a handful of animal and human studies that have identified chronic pain-induced microglial activation in discrete regions of the brain, including the ventral tegmental area (VTA), nucleus accumbens, amygdala, and rostroventral medulla (Huang et al, 2014; Sawada et al, 2014; Taylor et al, 2015; Roberts et al, 2009; Loggia et al, 2015), there has not yet been a systematic study to assess simultaneous microglial activation in brain regions involved in sensory and affective dimensions of pain. To this aim, we have assessed microglial activation in ipsilateral and contralateral brain regions associated with pain and affect in a mouse model of neuropathic pain.

Materials and Methods

Animals

A total of 34 male, C57Bl/6 mice (The Jackson Laboratory), 8–10 weeks of age, were housed in groups of four on a 12 hour light/dark cycle with food and water available *ad libitum*. No animals were excluded from analysis in any of the behavioral or molecular assays. All procedures were conducted in accordance with the National Institutes of Health *Guide for the Care of Use of Laboratory Animals* and were approved by the University of California-Los Angeles and the University of California-Irvine Institutional Animal Care and Use Committees.

Peripheral Nerve Injury

Animals were randomly assigned into two surgery groups, sham or peripheral nerve injury (PNI). Surgery was performed as described previously (Taylor et al, 2015; Mosconi and

Kruger, 1996). All animals were anesthetized with gaseous isoflurane (induction at 5% and maintenance at 2.5% in oxygen). For the PNI, an incision was made in the lateral left thigh followed by a blunt dissection of the left lateral thigh to expose the sciatic nerve. The nerve was encased with a polyethylene tubing (PE50, 2 mm long). The control group (sham surgery) received a similar surgery without dissection of the nerve. Animals were allowed to recover in their homecages for 2 weeks.

Behavior (von Frey)

Two weeks following nerve injury, mice were placed in a 10× 10 cm plexiglass box atop a wire mesh floor (n=6 per group, based on previous experience with this technique (Taylor et al, 2015)). After 30 minutes of acclimation to the environment, mechanical thresholds were assessed in the ipsilateral (left) paw of sham and PNI animals. Von Frey filaments of incremental stiffness were applied and a positive reaction was recorded following vigorous retraction of the hindpaw. The up-and-down method (Dixon, 1991) was used to measure the 50% withdrawal threshold (Chaplan et al, 1994). Withdrawal thresholds were averaged between groups and compared using a Mann-Whitney test, and significance set at $p<0.05$.

Immunocytochemistry

To assess PNI-induced microglial activation, tissue was processed for immunocytochemistry two weeks following nerve injury surgery. This time point was selected as we have previously shown it to correlate with peak pain behavior and robust microglial activation in the VTA (Taylor et al, 2014). Animals (n=6 per group) were were transcardially perfused with 4% paraformadlehyde (PFA) in 0.1M phosphate buffer (PB). The brain was dissected from the skull and postfixed in 30% sucrose before cryosectioning at 50um. Whole brains were divided into left and right hemispheres, and coronal sections were collected in 0.1M phosphate buffered saline with 0.2% Triton X 100 (PBS-T), incubated with blocking buffer (5% normal goat serum) for one hour prior to immunolabeling for microglia using an anti-IBA-1 antibody (1:2000; ionized calcium binding adaptor molecule; rabbit polyclonal; Wako, Cat# 016-20001, RRID:AB_839506; previously validated (Imai et al, 1996). Labeling was visualized using a goat anti-rabbit IgG conjugated to Alexa Fluor 488 (1:1000; Invitrogen). For analysis, images were acquired on an Olympus BX51 fluorescent microscope with 20× objective. Microglial activation was quantified by measuring cell body size using ImageJ software. This technique has been validated against our previous methods using defined qualitative criteria to assess activation (Taylor et al, 2015; Taylor et al, 2016; Kozlowski and Weimer, 2012). At least 20 cells over 3 separate slices per region per animal were measured and averaged to give a single value per animal. An experimenter blind to condition performed the imaging and quantification. For statistical analysis, means and standard error of the mean (SEM) were calculated per group, and compared using a 2-way ANOVA followed by Bonferonni post hoc analysis for comparing surgery and side. Differences were considered statistically different with $p<0.05$.

Real-time Quantitative PCR

Brains were collected from sham and PNI mice (5 per group) 8 weeks post149 surgery and were coronal-sectioned via cryostat (150 μm thick) at −20 °C and mounted on SuperFrost charged slides. Tissue punches (1 mm diameter) were taken using a disposable biopsy

plunger (Miltex, York, PA) for medial prefrontal cortex (mPFC), nucleus accumbens (NAc), bed nucleus stria terminalis (BNST), amygdala, hippocampus, thalamus, ventral tegmental area (VTA), and dorsal raphe nucleus (DRN). Because the nerve injury was performed in only the left hind leg of the mouse, brain tissue regions from the left and right hemispheres were assessed separately.

Total RNA was collected from the brain tissue punches via Trizol extraction method (Ambion Life Technologies, Grand Island, NY). RNA was converted to cDNA using 100 U of M-MulV Reverse Transcriptase, 1 μM Oligo d(T) $_{23}$VN, and 2 mM dNTP mix (New England Biolabs, Ipswich, MA), annealed at 70 °C and inactivated at 95 °C. Real-time qPCR was conducted using primer sets for IBA-1(using primers *Iba1*: Iba1-F: ATC AAC AAG CAA TTC CTC GAT GA, Iba1R: CAG CAT TCG CTT CAA GGA CAT A) and beta-actin (using primers for *actb* as a control gene (Actb-F: GGC TGT ATT CCC CTC CAT CG, Actb-R: CCA GTT GGT AAC AAT GCC ATG T). Using, 96-well optical plates (Applied Biosystems, Singapore), cDNA and PerfeCTa SYBR Green FastMix containing the primer sets (Quanta Biosciences, Gaithersburg, MD) were loaded and run on ABI ViiA7 fast block qPCR machine using cycling conditions in the PerfeCTa SYBR Green FastMix manual. Cycle threshold outputs were calculated and normalized to the actin housekeeping gene to compute Δ CT. Relative expression levels were determined by normalizing sham and PNI groups to actin control via Δ CT method. The results expressed as relative expression (2^Δ PCT). The means and SEM were statistically analyzed using one-way ANOVA with Bonferroni correction between sham and PNI brain regions. A $p < 0.05$ was considered significant.

Results

PNI resulted in a sustained pain state two weeks following surgery, as indicated by a significant reduction in mechanical withdrawal thresholds (sham: 0.91 g ± 0.10 versus 0.14 g ± 0.04, p=0.002, with a Mann-Whitney comparison, n=6 per group).

Iba-1 gene expression was significantly increased in neuropathic pain compared to sham animals, especially in the hemisphere of the brain contralateral to the nerve injured leg (Table 1, n=5 per group). Because primary nociceptive afferents decussate at the level of the spinal cord, injured afferent inputs are represented on the contralateral hemisphere of the brain. In particular, we observed significant increases in contralateral Iba-1 gene expression in the NAc (~2-fold) ($F_{(1,16\ side)} = 49.74$, ****$p<0.0001$, $F_{(1,16\ injury)} = 21.59$, ***$p<0.001$, and $F_{(1,16\ interaction)} = 8.071$, *$p<0.05$), the VTA (3.6-fold) ($F_{(1,16\ side)} = 6.1787$, p=0.175, $F_{(1,16\ injury)} = 41.74$, **$p<0.01$ and $F_{(1,16\ interaction)} = 2.912$, p=2.91) and the thalamus (2.6-fold) ($F_{(1,16\ side)} = 5.954$, p=0.099, $F_{(1,16\ injury)} = 45.84$, ***$p<0.001$, and $F_{(1,16\ interaction)} = 17.19$, **$p<0.01$) of the PNI group (Figure 1).

Similar to the qRT-PCR data, significant increases in microglial cell body size as determined by IBA-1 immunolabeling was evident in many brain regions important for both sensory and affective pain transmission (Table 2 and Figure 2, n=6 per group). In most regions, microglial cell body size was significantly greater on the contralateral, but not ipsilateral, side of the PNI group. In particular, we noted significant increase in cell body size in several

somatotopic regions of the primary sensory cortex, including the region corresponding to the hindlimb ($F_{(1,10\ side)}$=0.18, p=0.30, $F_{(1,10\ injury)}$=64.48, ***p<0.0001, $F_{(1,10\ interaction)}$=14.39, **p<0.01) and head ($F_{(1,10\ side)}$=6.26, p=0.09, $F_{(1,10\ injury)}$=0.58, p=0.46, $F_{(1,10\ interaction)}$=7.13, *p<0.05). We also noted significant unilateral microglial activation in the habenula ($F_{(1,10\ side)}$=13.72, **p<0.01, $F_{(1,10\ injury)}$=5.85, *p<0.05, $F_{(1,10\ interaction)}$=2.55, p=0.14), and VTA ($F_{(1,10\ side)}$=26.96, **p<0.01, $F_{(1,10\ injury)}$=3.98, p=0.07, $F_{(1,10\ interaction)}$=10.68, **p<0.008). Interestingly, the nucleus accumbens showed microglial activation on both the contralateral and ipsilateral side in the peripheral nerve injury group ($F_{(1,10\ side)}$=0.29, p=0.59, $F_{(1,10\ injury)}$=10.25, **p<0.01, $F_{(1,10\ interaction)}$=0.33, p=0.57). The motor cortex did not show any change in microglial morphology on either side in the peripheral nerve injury group ($F_{(1,10\ side)}$=2.45, p=0.15, $F_{(1,10\ injury)}$=0.07, p=0.79, $F_{(1,10\ interaction)}$=0.56, p=0.47). No change in microglial cell body size was observed in either the ipsilateral or contralateral side of the sham group. Total number of microglial cells did not differ between sham and PNI groups, nor ipsilateral or contralateral sides in any of the brain regions measured (data not shown).

Discussion

Here we've shown that a peripheral nerve lesion results in significant microglial activation in brain regions associated with pain and affect, including the thalamus, prefrontal cortex, and several limbic regions. This complements previous studies demonstrating robust microglial activation in the spinal cord following nerve injury, and suggests pain-induced neuroinflammation occurs widely throughout the neuroaxis (Taves et al., 2016; Li et al., 2016). This premise is supported by a previous study which found chemotherapy-induced pain resulted in significant microglial activation throughout many brain regions including the PAG, thalamus, anterior cingulate cortex, secondary sensory cortex and medium forebrain bundle (Di Cesare Mannelli et al, 2013). The current study extends these results by showing that even pain of a peripherally restricted origin is capable of activating microglia in diverse regions of the central nervous system. Notably, a recent study examining chronic pain patients has reported evidence for microglial activation in several of the same brain regions described in our current study, including the thalamus and sensory cortical regions (Loggia et al, 2015). Taken together, these studies form an emerging perspective recognizing brain microglia as a key mechanism in the progression of chronic pain phenotypes.

It should be noted that an earlier study observed no microglial activation in higher cortical regions following a peripheral nerve injury (Zhang et al, 2008). The lack of microglial activation in this study could be due to the use of transgenically-labelled microglia (CX3CR1-GFP), Given this line exhibits only one functional copy of the CX3CR1 receptor, impairments in pain-induced microglial activation might be expected (Jung et al, 2000). This would be particularly true in the brain, where the degree of microglial activation is not as robust as is observed in the ipsilateral spinal cord.

The wide range of brain regions in which microglial activation was detected raises the question as to what signals or mechanisms are responsible for pain-induced microglial activation at sites far removed from the site of injury. Of note is the observation that the peripheral nerve injury did not induce microglial activation in all brain regions, such as the

motor cortex. Moreover, in regions in which significant microglial activation was observed, the effect was always highest on the contralateral side. Because nociceptive afferents decussate at the level of the spinal cord, injured afferent inputs would be expected on the contralateral side. These observations suggest that microglial activation is driven by cues relating to injured-afferent input, though what these specific signals are is a question that remains to be answered.

The breadth of microglial activation throughout the brain suggests a potential for influencing pain progression in a variety of brain regions. The research delineating the mechanisms by which microglia influence pain behavior in a region specific manner is in its infancy. We have recently shown that microglial activation in the VTA impairs dopamine neuron activity and opioid reward via a BDNF-KCC2 pathway (Taylor et al, 2015). In the amygdala, CCR2 and IL1beta were implicated in the development of pain-induced anxiety (Sawada et al, 2014). Given the robust activation of microglia that we observed in several brain regions, further research is warranted to identify novel areas in which microglia contribute to the development and progression of chronic pain.

Acknowledgments

The authors would like to thank Chris Evans for institutional support. Financial support was provided by NIHK99DA040016 (AMWT), DOD MR141282 (CMC), The Shirley and Stefan Hatos Foundation (AMWT, CMC, SM), Shirley Hatos (CMC), and the Cousins Center for Psychoneuroimmunology (AMWT).

Reference List

Asmundson GJ, Katz J. Understanding the co-occurrence of anxiety disorders and chronic pain: state-of-the-art. Depression and anxiety. 2009; 26(10):888–901. [PubMed: 19691031]

Bhattacharya A, Derecki NC, Lovenberg TW, Drevets WC. Role of neuro-immunological factors in the pathophysiology of mood disorders. Psychopharmacology. 2016; 233(9):1623–1636. [PubMed: 26803500]

Chaplan SR, Bach FW, Pogrel JW, Chung JM, Yaksh TL. Quantitative assessment of tactile allodynia in the rat paw. J Neurosci Methods. 1994; 53(1):55–63. [PubMed: 7990513]

Di Cesare Mannelli L, Pacini A, Bonaccini L, Zanardelli M, Mello T, Ghelardini C. Morphologic features and glial activation in rat oxaliplatin-dependent neuropathic pain. Journal of Pain. 2013; 14(12):1585–1600. [PubMed: 24135431]

Dixon WJ. Staircase Bioassay: The Up-and-Down Method. Neuroscience and biobehavioral reviews. 1991; 15:47–50. [PubMed: 2052197]

Elman I, Borsook D, Volkow ND. Pain and suicidality: insights from reward and addiction neuroscience. Progress in neurobiology. 2013; 109:1–27. [PubMed: 23827972]

Huang ZX, Lu ZJ, Ma WQ, Wu FX, Xhang YQ, Yu WF, Zhao ZQ. Involvement of RVM-expressed P2X7 receptor in bone cancer pain: mechanism of descending facilitation. Pain. 2014; 155(4):783–791. [PubMed: 24447511]

IASP. Part II: Pain Terms, A Currents List with Definitions and Notes on Usage. In: Merskey, H., Bogduk, N., editors. Classification of chronic pain. Seattle: IASP Press; 1994. p. 209-214.

Imai Y, Ibata I, Ito D, Ohsawa K, Kohsaka S. A Novel Gene iba1 in the Major Histocompatability Complex Class II Region Encoding an EF Hand Protein Expressed in a Monocytic Lineage. Biochem Biophys Res Comm. 1996; 224(855–862)

Jung S, Aliberti J, Graemmel P, Sunshine MJ, Kreutzberg GW, Sher A, Littman DR. Analysis of fractalkine receptor CX(3)CR1 function by targeted deletion and green fluorescent protein reporter gene insertion. Molecular and cellular biology. 2000; 20(11):4106–4114. [PubMed: 10805752]

Juurlink DN, Hermann N, Szalai JP, Kopp A, Redelmeier DA. Medical Illness and the Risk of Suicide in the Elderly. Archives of internal medicine. 2004; 164:1179–1184. [PubMed: 15197042]

Keller AF, Beggs S, Salter MW, De Koninck Y. Transformation of the output of spinal lamina I neurons after nerve injury and microglia stimulation underlying neuropathic pain. Molecular pain. 2007; 3:27. [PubMed: 17900333]

Kozlowski C, Weimer RM. An automated method to quantify microglia morphology and application to monitor activation state longitudinally in vivo. PloS one. 2012; 7(2):e31814. [PubMed: 22457705]

Ledeboer A, Sloane EM, Milligan ED, Frank MG, Mahony JH, Maier SF, Watkins LR. Minocycline attenuates mechanical allodynia and proinflammatory cytokineexpression in rat models of pain facilitation. Pain. 2005; 115(1–2):71–83. [PubMed: 15836971]

Li Z, Wei H, Piirainen S, Chen Z, Kalso E, Pertovaara A, Tian L. Spinal versusbrain microglial and macrophage activation traits determine the differential neuroinflammatory responses and analgesic effect of minocycline in chronicneuropathic pain. Brain Behav Immun. 2016 In press.

Loggia ML, Chonde DB, Akeju O, Arabasz G, Catana C, Edwards RR, Hill E, Hsu S, Izquierdo-Garcia D, Ji RR, Riley M, Wasan AD, Zurcher NR, Albrecht DS, Vangel MG, Rosen BR, Napadow V, Hooker JM. Evidence for brain glial activation in chronic pain patients. Brain. 2015; 138(Pt 3):604–615. [PubMed: 25582579]

Mika J, Rojewska E, Makuch W, Przewlocka B. Minocycline reduces the injury-induced expression of prodynorphin and pronociceptin in the dorsal root ganglion in a rat model of neuropathic pain. Neuroscience. 2010; 165(4):1420–1428. [PubMed: 19961904]

Mosconi T, Kruger L. Fixed-diameter polyethylene cuffs applied to the rat sciatic nerve induce a painful neuropathy: ultrastructural morphometric analysis of axonal alterations. Pain. 1996; 64:37–57. [PubMed: 8867246]

Nicholson B, Verma S. Comorbidities in chronic neuropathic pain. Pain Medicine. 2004; 5(S1):S9–S27. [PubMed: 14996227]

Raghavendra V, Tanga F, DeLeo JA. Inhibition of microglial activation attenuates the development but not existing hypersensitivity in a rat model of neuropathy. J Pharmacol Exp Ther. 2003; 306(2): 624–630. [PubMed: 12734393]

Roberts J, Ossipov MH, Porreca F. Glial activation in the rostroventromedial medulla promotes descending facilitation to mediate inflammatory hypersensitivity. The european journal of neuroscience. 2009; 30(2):229–241. [PubMed: 19614984]

Sawada A, Niiyama Y, Ataka K, Nagaishi K, Yamakage M, Fujimiya M. Suppression of bone marrow-derived microglia in the amygdala improves anxiety-like behavior induced by chronic partial sciatic nerve ligation in mice. Pain. 2014; 155(9):1762–1772. [PubMed: 24907405]

Taves S, Berta T, Liu DL, Gan S, Chen G, Kim YH, Van de Ven T, Laufer S, Ji RR. Spinal inhibition of p38 MAP kinase reduces inflammatory and neuropathic pain in male but not female mice: Sex-dependetn microglial signaling in the spinal cord. Brain Behav Immun. 2016; 55:70–81. [PubMed: 26472019]

Taylor AMW, Murphy NP, Evans CJ, Cahill CM. Correlation Between Ventral Striatal Catecholamine Content and Nociceptive Thresholds in Neuropathic Mice. Journal of Pain. 2014; 15(8):878–885. [PubMed: 25052072]

Taylor AM, Castonguay A, Taylor AJ, Murphy NP, Ghogha A, Cook C, Xue L, Olmstead MC, De Koninck Y, Evans CJ, Cahill CM. Microglia disrupt mesolimbic reward circuitry in chronic pain. J Neurosci. 2015; 35(22):8442–8450. [PubMed: 26041913]

Taylor AM, Castonguay A, Ghogha A, Vayssiere P, Pradhan AA, Xue L, Mehrabani S, Wu J, Levitt P, Olmstead MC, De Koninck Y, Evans CJ, Cahill CM. Neuroimmune Regulation of GABAergic Neurons Within the Ventral Tegmental Area During Withdrawal from Chronic Morphine. Neuropsychopharmacology. 2016; 41(4):949–959. [PubMed: 26202104]

Tsuda M, Inoue K. Neuron-microglia interaction by purinergic signaling in neuropathic pain following neurodegeneration. Neuropharmacology. 2015; 104:76–81. [PubMed: 26327676]

Zhang F, Vadakkan KI, Kim SS, Wu LJ, Shang Y, Zhuo M. Selective activation of microglia in spinal cord but not higher cortical regions following nerve injury in adult mouse. Molecular pain. 2008; 4:15. [PubMed: 18423014]

Significance Statement

Here we show that a peripherally restricted chronic pain stimulus is capable of robustly activating central immune cells widely throughout the brain, particularly in regions associated with pain and affect. Thus, the potential effects of activated microglia are wide ranging with respect to chronic pain behaviors.

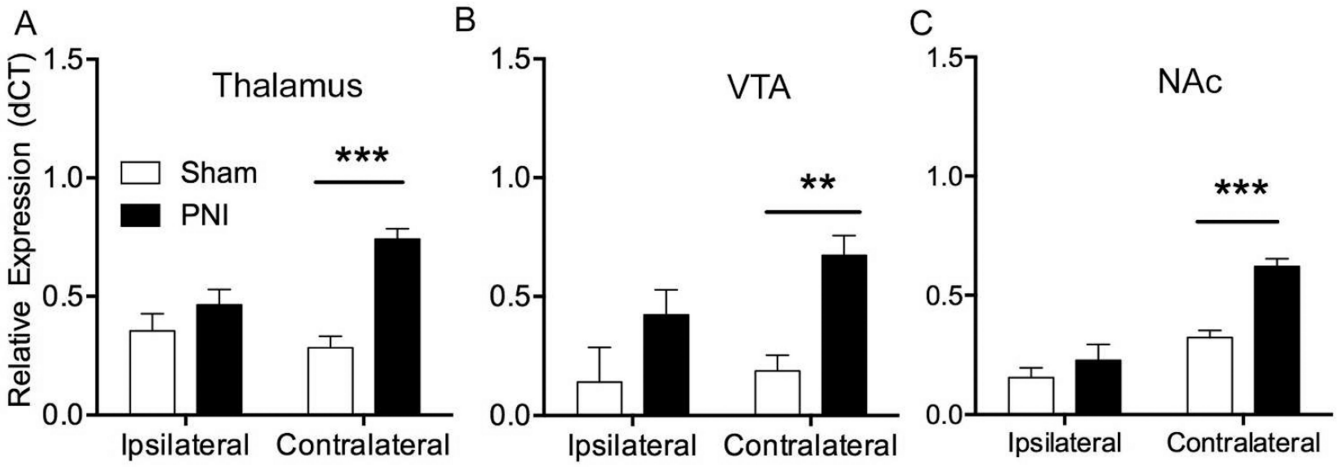

Figure 1.

Representative brain regions showing upregulation of IBA-1 mRNA following peripheral nerve injury (PNI). Expression levels of the IBA-1 mRNA was measured by qRT-PCR from brain regions both ipsilateral and contralateral to surgery. Data are transformed to relative expression (2^dCT). Error bars show the SEM. Abbreviations: VTA, ventral tegmental area. NAc, nucleus accumbens. **=p<0.01, ***=p<0.001.

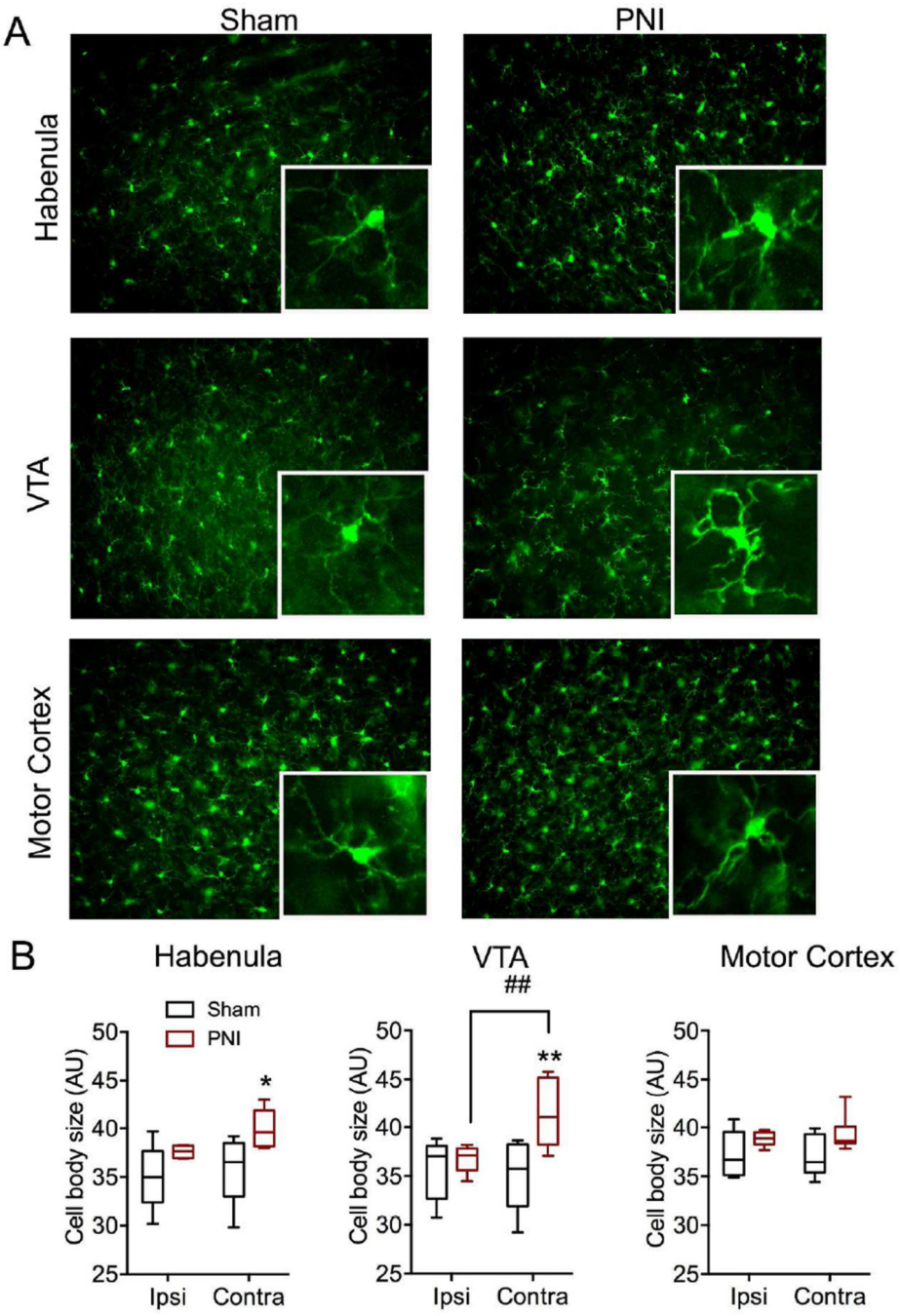

Figure 2.

Representative brain regions showing changes in microglial morphology following peripheral nerve injury (PNI). A) Representative fluorescent micrographs taken with a 20× objective from contralateral habenula, VTA, and motor cortex sections of sham and PNI animals labeled with IBA-1. Inset represents magnification of larger image. For scale, inset box = 100μm×100μm B) Quantification of average microglial cell body size from sham and PNI groups in select brain regions. Data expressed as box and whiskers plot with whiskers representing minimum and maximum values. Abbreviations: VTA, ventral tegmental area;

ipsi, ipsilateral; contra, contralateral. *=p<0.05, **=p<0.01 when compared to ipsilateral side of same group; ##=p<0.01 when compared to contralateral side of sham group.

Table 1

IBA1 mRNA levels in isolated brain regions of control (sham) and peripheral nerve injury (PNI) groups.

Brain Region	Sham		PNI	
	Ipsilateral	Contralateral	Ipsilateral	Contralateral
mPFC	0.13 (0.07)	0.06 (0.03)	0.12 (0.12)	0.17 (0.1)
NAc	0.15 (0.04)	0.32 (0.03)	0.23 (0.07)	0.62 (0.03) ****, ##, ϕ*
BNST	0.14 (0.08)	0.14 (0.05)	0.42 (0.02)	0.74 (0.06) ***, ###, ϕ*
Amygdala	0.62 (0.05)	0.54 (0.06)	0.71 (0.04)	1.21 (0.07) ****, ###, ϕϕϕ*
Hippocampus	0.31 (0.19)	0.36 (0.02)	0.15 (0.05)	0.12 (0.06)
Thalamus	0.35 (0.07)	0.28 (0.05)	0.47 (0.07)	0.74 (0.04) **, ###, ϕϕ*
VTA	0.14 (0.14)	0.19 (0.07)	0.42 (0.11)	0.67 (0.08) #

Data is expressed as relative expression normalized to beta actin (2^dCT).

Abbreviations: PFC, prefrontal cortex; NAc, nucleus accumbens; BNST, bed nucleus stria terminalis; VTA, ventral tegmental area.

**** =p<0.01,

***** =p<0.001 compared to ipsilateral side of same condition,

=p<0.05,

=p<0.01,

=p<0.001 compared to sham contralateral side,

ϕ =p<0.05,

ϕϕ =p<0.01,

ϕϕϕ =p<0.001 interaction between side and treatment.

Table 2

Microglial cell body size in isolated brain regions of control (sham) and peripheral nerve injury (PNI) groups.

Brain Region	Sham		PNI	
	Ipsilateral	Contralateral	Ipsilateral	Contralateral
S1-J	36.7 (0.64)	38.0 (1.37)	36.25 (0.67)	38.84 (0.63) **, ϕ
S1-HL	35.5 (0.76)	34.1 (0.74)	39.7 (0.7)	42.3 (0.50) *, ϕϕ
MC-J	36.9 (0.75)	37.2 (0.79)	38.8 (0.59)	39.3 (0.59)
MC-HL	36.0 (0.44)	32.5 (0.77)	33.7 (0.64)	31.6 (1.01)
NAc	35.7 (0.67)	35.6 (0.37)	37.7 (0.72) #	38.5 (0.69) #
Amygdala	38.1 (0.3)	35.1 (0.80)	35.6 (0.52)	38.45 (1.56)
Habenula	35.0 (1.51)	35.9 (1.60)	37.6 (0.24)	39.9 (0.79) **, #
PAG	35.5 (2.14)	36.2 (1.34)	38.4 (0.45)	40.3 (0.83) *, #
VTA	35.7 (1.41)	35.2 (1.67)	36.8 (0.56)	41.4 (1.47) **, #, ϕϕ

Data is expressed as average cell body size (in arbitrary units) with S.E.M in parentheses.

Abbreviations: S1-J, primary sensory cortex (Jaw); S1HL, primary sensory cortex (hind limb); MC-J, motor cortex (jaw); MC-HL, motor cortex (hind limb); NAc, nucleus accumbens; PAG, periaqueductal grey; VTA, ventral tegmental area.

*=p<0.05,

**=p<0.01 compared to ipsilateral side of same condition,

#=p<0.05, compared to sham contralateral side,

ϕ=p<0.05,

ϕϕ=p<0.01 interaction between side and treatment.